Characterization of the ATP4 ion pump in *Toxoplasma gondii*

Received for publication, November 13, 2018, and in revised form, January 31, 2019 Published, Papers in Press, February 5, 2019, DOI 10.1074/jbc.RA118.006706

Adele M. Lehane[‡1,2], Adelaide S. M. Dennis[‡1], Katherine O. Bray[‡], Dongdi Li[‡], Esther Rajendran[‡], James M. McCoy[§¶], Hillary M. McArthur[‡], Markus Winterberg[‡3], Farid Rahimi[‡], Christopher J. Tonkin[§¶], Kiaran Kirk[‡4], and Giel G. van Dooren[‡5]

From the [‡]Research School of Biology, Australian National University, Canberra, ACT 2601, Australia, the [§]Walter and Eliza Hall Institute of Medical Research, Melbourne, VIC 3052, Australia, and the [¶]Department of Medical Biology, University of Melbourne, Melbourne, VIC 3010, Australia

Edited by Roger J. Colbran

The *Plasmodium falciparum* ATPase *Pf*ATP4 is the target of a diverse range of antimalarial compounds, including the clinical drug candidate cipargamin. *Pf*ATP4 was originally annotated as a Ca^{2+} transporter, but recent evidence suggests that it is a Na^+ efflux pump, extruding Na^+ in exchange for H^+. Here we demonstrate that ATP4 proteins belong to a clade of P-type ATPases that are restricted to apicomplexans and their closest relatives. We employed a variety of genetic and physiological approaches to investigate the ATP4 protein of the apicomplexan *Toxoplasma gondii*, *Tg*ATP4. We show that *Tg*ATP4 is a plasma membrane protein. Knockdown of *Tg*ATP4 had no effect on resting pH or Ca^{2+} but rendered parasites unable to regulate their cytosolic Na^+ concentration ($[Na^+]_{cyt}$). *Pf*ATP4 inhibitors caused an increase in $[Na^+]_{cyt}$ and a cytosolic alkalinization in WT but not *Tg*ATP4 knockdown parasites. Parasites in which *Tg*ATP4 was knocked down or disrupted exhibited a growth defect, attributable to reduced viability of extracellular parasites. Parasites in which *Tg*ATP4 had been disrupted showed reduced virulence in mice. These results provide evidence for ATP4 proteins playing a key conserved role in Na^+ regulation in apicomplexan parasites.

The Apicomplexa are a phylum of unicellular parasitic protists that impose enormous medical, veterinary, and socioeconomic burdens. Members of this phylum include *Plasmodium*, multiple species of which cause malaria in humans, and *Toxoplasma gondii*, the causative agent of toxoplasmosis. Apicomplexan parasites have complex life cycles that involve intracellular and extracellular stages, often in at least two different host organisms, in which they encounter vastly different external environments. To survive, they must regulate their cytosolic Na^+ concentration ($[Na^+]_{cyt}$) and pH (pH_{cyt}) in the face of widely varying external ionic conditions. How they accomplish this is not well understood.

Cells typically control their $[Na^+]_{cyt}$ and pH_{cyt} tightly, using a variety of membrane transporters and channels to do so. Differences between extracellular and intracellular Na^+ and H^+ concentrations (*i.e.* ion gradients) are exploited for essential processes such as nutrient acquisition and cell volume regulation. In most cell types, the cytosol is typically slightly alkaline (pH ~7.2–7.3), and the $[Na^+]_{cyt}$ is typically around 10 mM (1, 2).

Most studies of Na^+ and pH regulation in apicomplexan parasites to date have been performed with the blood-stage form of the most virulent human malaria parasite, *Plasmodium falciparum*. This parasite has, on its plasma membrane, a H^+-extruding V-type ATPase that plays a key role in pH regulation (3, 4) while also generating a large, inwardly negative membrane potential (5). The extracellular tachyzoite form of *T. gondii* has also been shown to have a plasma membrane V-type H^+-ATPase that plays roles both in controlling pH_{cyt} and generating and maintaining the membrane potential (6).

Na^+ regulation in apicomplexan parasites has recently emerged as an area of particular interest. In an attempt to identify the target of a promising new class of antimalarials, the "spiroindolones," *P. falciparum* parasites were exposed to increasing sublethal doses of these drugs *in vitro* until parasites showing low-level resistance emerged. Resistant parasites were found to have mutations in *PfATP4*, a gene encoding a plasma membrane P-type ATPase (7). *Pf*ATP4 was originally annotated as a Ca^{2+} transporter (8); however, there are now multiple lines of evidence that the transporter mediates the efflux of Na^+ from the parasite. First, antiplasmodial spiroindolones (of which cipargamin, formerly known as NITD609 and KAE609, is the clinical candidate) cause a rapid increase in the parasite's $[Na^+]_{cyt}$ and Na^+ content (9–11). The same is true of a range of structurally unrelated antiplasmodial agents for which mutations in *Pf*ATP4 confer resistance (12–15). Second, spiroindolone-resistant parasites with mutations in *Pf*ATP4 are less

This work was supported by National Health and Medical Research Council Grant 1042272 (to K. K.) and Australian Research Council Discovery Project Grant DP150102883 (to K. K. and G. G. v. D.), Linkage Project Grant LP150101226 (to K. K.), Discovery Early Career Researcher Award DE160101035 (to A. M. L.), QEII Fellowship DP110103144 (to G. G. v. D.), and Future Fellowship FT120100164 (to C. J. T.). C. J. T. is grateful for institutional support from the Victorian State Government Operational Infrastructure Support Program and the National Health and Medical Research Council Independent Research Institute Infrastructure Support Scheme. The authors declare that they have no conflicts of interest with the contents of this article.

This article contains Figs. S1–S5.

[1] Both authors contributed equally to this work.

[2] To whom correspondence may be addressed: Tel.: 61-2-6125-6970; E-mail: adele.lehane@anu.edu.au.

[3] Present address: Centre for Tropical Medicine and Global Health, Nuffield Dept. of Medicine, University of Oxford, UK and Mahidol-Oxford Tropical Medicine Research Unit, Faculty of Tropical Medicine, Mahidol University, Bangkok, Thailand.

[4] To whom correspondence may be addressed. Tel.: 61-2-6125-0421; E-mail: kiaran.kirk@anu.edu.au.

[5] To whom correspondence may be addressed. Tel.: 61-2-6125-0665; E-mail: giel.vandooren@anu.edu.au.

sensitive to the disruption of $[Na^+]_{cyt}$ by spiroindolones and also have a higher resting $[Na^+]_{cyt}$, consistent with resistance-conferring mutations in *Pf*ATP4 causing some impairment of its Na^+ transport function (10, 13). Third, spiroindolones inhibit Na^+-dependent ATPase activity in parasite membrane preparations (10, 16, 17).

In addition to dissipating the Na^+ gradient across the plasma membrane of the malaria parasite, spiroindolones and other "*Pf*ATP4-associated" antimalarials cause an increase in pH_{cyt}, *increasing* the pH gradient across the parasite plasma membrane (10, 13–16, 18). *Pf*ATP4 has been postulated to expel Na^+ from the parasite in exchange for H^+, imposing a significant "acid load" on the parasite (19). Lifting this load by inhibiting *Pf*ATP4 results in a cytosolic alkalinization.

The disruption of ion regulation by the *Pf*ATP4-associated antimalarials triggers a variety of detrimental events in the parasite (9, 20). It is not known whether ATP4 homologues in other apicomplexan parasites are similarly vulnerable.

Little is known about Na^+ regulation in *T. gondii*. The plasma membrane of *T. gondii* harbors two candidate Na^+/H^+ exchangers, *Tg*NHE1 and *Tg*NHE4 (21, 22). pH_{cyt} is unaffected by the removal of extracellular Na^+ (6) and is unchanged in mutant parasites lacking a functional *Tg*NHE1 (21), consistent with *Tg*NHE1 not playing a significant role in the maintenance of the parasite's resting pH_{cyt}. *Tg*NHE1 mutant parasites have an elevated $[Ca^{2+}]_{cyt}$, suggesting a role for *Tg*NHE1 in Ca^{2+} regulation, perhaps via an effect on $[Na^+]_{cyt}$ (21). However, the $[Na^+]_{cyt}$ of *T. gondii* has not been studied directly. The antimalarial spiroindolone cipargamin has been shown to inhibit the growth of *T. gondii* (23), raising the possibility that the *T. gondii* homolog of ATP4 (*Tg*ATP4) may play an important role in this parasite. However, neither the function of *Tg*ATP4 nor the sensitivity of *Tg*ATP4 to cipargamin have been investigated.

In this study, we used a combination of genetic and physiological approaches to provide evidence that *Tg*ATP4 is a plasma membrane Na^+ pump that is important for Na^+ homeostasis, particularly in extracellular parasites that encounter high $[Na^+]$, and sensitive to a number of compounds that are believed to target *Pf*ATP4.

Results

The apicomplexan ATP4 proteins form a distinct subfamily of type II P-type ATPases

*Tg*ATP4 (TGME49_278660) shares significant sequence similarity with *Pf*ATP4 (Fig. S1). *Tg*ATP4 and *Pf*ATP4 both contain the eight semiconserved regions that have been described as comprising the "core of the P-type ATPase superfamily" (24), as well as the PROSITE consensus sequence for the phosphorylation site of P-type ATPases, D-K-T-G-T-[LIVM]-[TI] (Fig. S1). *Pf*ATP4 belongs to the type II branch of P-type ATPases (24), which includes ATP-driven Ca^{2+}, Na^+, K^+, and H^+ transporters. Type II P-type ATPases have been previously divided into four subgroups (A–D) based on a phylogenetic analysis of their 265-residue "core" region (24). Type IIA and type IIB P-type ATPases transport Ca^{2+}, whereas type IIC P-type ATPases include Na^+/K^+ transporters and H^+/K^+ transporters (24). Type IID P-type ATPases are "*exitus natrus*" (ENA)[6] transporters that have been proposed to extrude Na^+ (24).

We performed a phylogenetic analysis of type II P-type ATPases with a dataset consisting of *Tg*ATP4; *Pf*ATP4; other type II P-type ATPases from *T. gondii*, *P. falciparum*, and other apicomplexans; and type II P-type ATPases from a range of other eukaryotes, including other members of the Alveolata (ciliates, dinoflagellates, and chromerids), the superphylum of eukaryotes to which apicomplexans belong. Our analysis revealed four previously defined subgroups of type II P-type ATPases (24) plus a fifth subgroup of proteins, referred to here as "ATP4-type ATPases" (Fig. 1). The ATP4-type ATPase subgroup has strong bootstrap support and includes *Tg*ATP4, *Pf*ATP4, and proteins from all other apicomplexans we examined. We also identified ATP4-type ATPases in the chromerids *Vitrella brassicaformis* and *Chromera velia* and in the dinoflagellate *Symbiodinium minutum*. Chromerids and dinoflagellates are the closest extant relatives of apicomplexans (25, 26), and the presence of ATP4-type ATPases encoded in the genomes of these organisms suggests that ATP4-type ATPases evolved before these three lineages diverged. The absence of ATP4-type ATPases in other eukaryotes suggests that this family of proteins is restricted to apicomplexans and closely related organisms.

TgATP4 localizes to the T. gondii plasma membrane and is important for parasite growth

To examine the expression and localization of *Tg*ATP4, we fused a HA tag to the 3′ end of the ORF of the gene. Western blotting revealed that the resultant *Tg*ATP4-HA protein had an approximate mass of 160 kDa (Fig. 2*A*), close to the predicted mass of 147 kDa for HA-tagged *Tg*ATP4. Immunofluorescence assays revealed that *Tg*ATP4 co-localized with a marker for the plasma membrane (P30; 27) (Fig. 2*B*).

To determine whether *Tg*ATP4 is important for *T. gondii* growth, we generated a *Tg*ATP4 inducible knockdown line in which the native *TgATP4* promoter was replaced with an anhydrotetracycline (ATc)-regulated promoter, and the resultant protein was fused with an N-terminal HA tag (Fig. S2, *A* and *B*). We refer to this strain as "iHA-*Tg*ATP4." We confirmed localization of the HA-*Tg*ATP4 protein to the plasma membrane in this strain (Fig. S2*C*).

Exposure of iHA-*Tg*ATP4 parasites to ATc led to down-regulation of HA-*Tg*ATP4 expression, with the protein becoming nearly undetectable by Western blotting (Fig. 2*C*) and in immunofluorescence assays (Fig. S2*C*) 2 days after the addition of ATc. To determine whether *Tg*ATP4 is important for parasite growth and survival, we introduced the bright tandem dimeric Tomato (tdTomato) red fluorescent protein into the iHA-*Tg*ATP4 strain (creating a strain we termed "iHA-*Tg*ATP4/Tomato"), allowing us to monitor parasite growth fluorometrically using an assay described previously (28). Addition of ATc at the start of the assay resulted in a decrease in the growth of iHA-

[6] The abbreviations used are: ENA, *exitus natrus*; ATc, anhydrotetracycline; ANOVA, analysis of variance; gRNA, guide RNA; SBFI, sodium-binding benzofuran isophthalate; BCECF, 2′,7′-bis-(2-carboxyethyl)-5-(and-6)-carboxyfluorescein; IFA, immunofluorescence assay.

Figure 1. Phylogenetic analysis of *Tg*ATP4. A phylogenetic tree of type II P-type ATPases shows the previously defined groups type IIA, B, C, and D and a new group, the ATP4-type ATPases. The latter group, shaded in *green*, includes *Pf*ATP4 and *Tg*ATP4 (indicated by *arrows*). The tree was created using maximum likelihood analysis of protein amino acid sequence using the phylogenetic software package PHYLIP. *PMCA*, plasma membrane Ca^{2+} ATPase; *SERCA*, sarco/endoplasmic reticulum Ca^{2+}-ATPase; *SPCA*, secretory pathway Ca^{2+}-ATPase.

*Tg*ATP4/Tomato parasites ($p < 0.05$, one-way ANOVA; Fig. 2*D*) but not in that of Tomato-expressing WT ("WT/Tomato") parasites ($p > 0.05$, one-way ANOVA; Fig. 2*D*). Addition of ATc to iHA-*Tg*ATP4/Tomato parasites 3 days before commencing the assay (and maintaining its presence throughout the assay) further exacerbated the growth defect ($p < 0.05$, one-way ANOVA; Fig. 2*D*). To determine whether these growth defects were specifically the result of *Tg*ATP4 knockdown, we complemented iHA-*Tg*ATP4/Tomato parasites with constitutively expressed Ty1-tagged *Tg*ATP4 (generating a strain we termed "iHA-*Tg*ATP4/Tomato/cTy1-*Tg*ATP4"). This restored parasite growth in the presence of ATc (Fig. 2*D*), indicating that the growth phenotype observed in the iHA-*Tg*ATP4/Tomato strain resulted exclusively from the lack of expression of *Tg*ATP4.

The requirement for *Tg*ATP4 expression at different stages of the lytic cycle of *T. gondii* was investigated using a series of assays. First we investigated whether *Tg*ATP4 expression was important for the growth of intracellular parasites. iHA-*Tg*ATP4/Tomato parasites and WT/Tomato parasites were incubated with or without ATc for 2 days, extracted from their host cells, and allowed to invade new host cells for 24 h. The number of parasites per host cell vacuole was then determined. Most vacuoles contained either eight or 16 parasites at this time point (Fig. 3*A*), and there were no significant differences in the percentage of host cell vacuoles having any given number of parasites between WT/Tomato and iHA-*Tg*ATP4/Tomato parasites or between ATc-treated and untreated parasites ($p > 0.05$, one-way ANOVA). These data suggest that *Tg*ATP4 expression is not required for the intracellular growth or division of *T. gondii*.

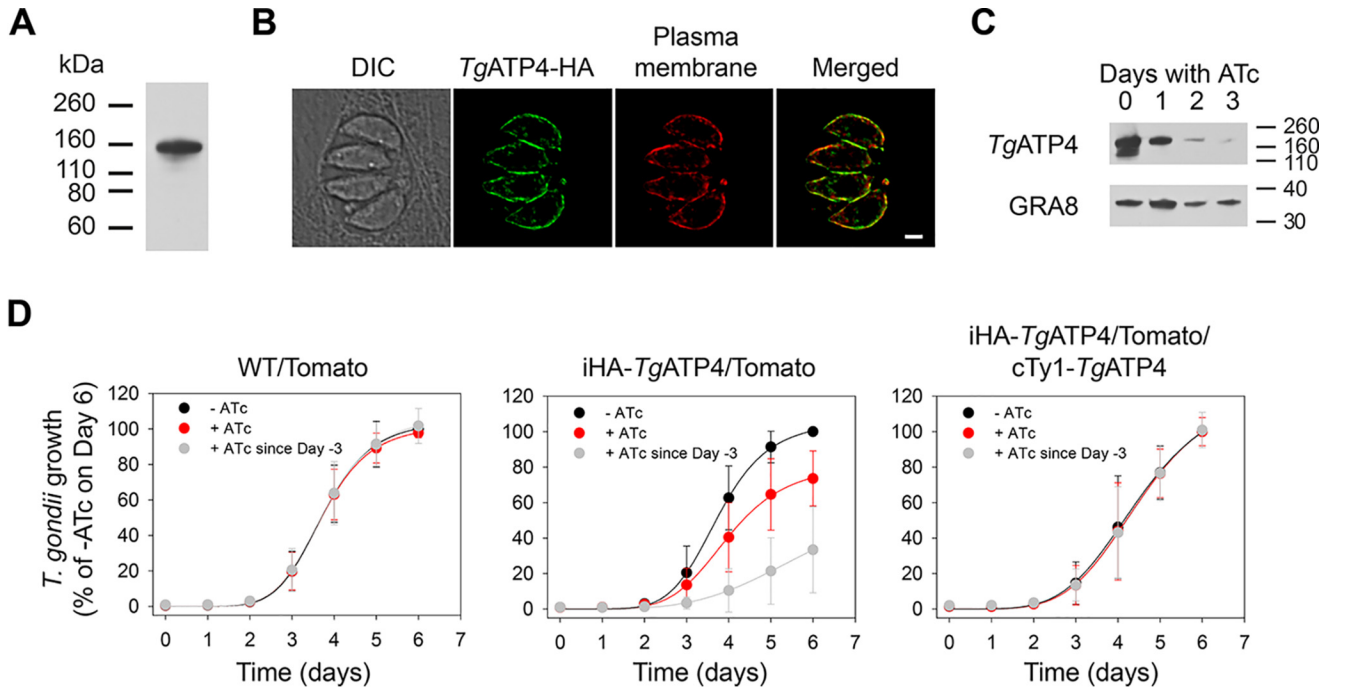

Figure 2. Localization of *Tg*ATP4 and the effect of down-regulating its expression on *T. gondii* growth. *A*, Western blotting of *Tg*ATP4-HA–expressing parasites performed using an anti-HA antibody. *B*, immunofluorescence assay of *Tg*ATP4-HA protein (*green*) reveals co-localization with the plasma membrane marker P30 (*red*). The *scale bar* represents 2 μm. *DIC*, differential interference contrast. *C*, Western blotting of iHA-*Tg*ATP4 parasites grown for 0–3 days on ATc. Parasite protein extracts were probed with anti-HA (*top*) and anti-GRA8, an antibody against a dense granule protein, as a loading control (*bottom*). *D*, growth of the WT/Tomato, iHA-*Tg*ATP4/Tomato, and iHA-*Tg*ATP4/Tomato/cTy1-*Tg*ATP4 parasites in the absence of ATc (*black symbols*), in the presence of ATc (from day 0, *red symbols*), and in the presence of ATc from 3 days before the start of the assay (*gray symbols*). The data show the mean ± S.D. of four independent experiments. For each parasite line and day (from Day 1 onward), the growth under the three different conditions was compared using a one-way ANOVA with blocking (see "Experimental procedures"). Statistically significant differences ($p < 0.05$) were only observed for the iHA-*Tg*ATP4/Tomato parasite line. For this line, the difference between the −ATc and +ATc since Day −3 conditions was statistically significant from Day 2 onward, and the difference between the −ATc and +ATc conditions was significant on Days 4 and 5. There was also a significant difference between the +ATc and "+ATc since Day −3 conditions on Days 2, 4, 5, and 6.

We next investigated whether knocking down *Tg*ATP4 impaired the ability of parasites to egress from their host cells. The egress of parasites from their host cells was stimulated by addition of the Ca^{2+} ionophore A23187, and "percent egress" (the percentage of individual parasitophorous vacuoles from which parasites were observed to escape) was calculated as described previously (29). No significant difference in the percent egress was observed between WT and iHA-*Tg*ATP4 parasites or between parasites maintained for 30 h in the presence or absence of ATc (Fig. 3*B*; $p > 0.05$, one-way ANOVA).

To investigate whether *Tg*ATP4 is important for invasion, WT/Tomato and iHA-*Tg*ATP4/Tomato parasites were grown in the absence or presence of ATc for 2 days and then allowed to invade host cells for 10 min. There was a small apparent decrease in invasion of iHA-*Tg*ATP4/Tomato parasites grown in the presence of ATc (Fig. 3*C*), but this decrease was not statistically significant ($p > 0.05$, one-way ANOVA). We conclude that the defect in overall parasite growth observed upon *Tg*ATP4 knockdown (Fig. 2*D*) cannot be explained by defects in invasion, egress, or intracellular growth (Fig. 3, *A*–*C*).

In preliminary experiments, we observed that extracellular iHA-*Tg*ATP4 parasites treated with ATc exhibited an altered, rounded morphology and frequently contained a large intracellular vacuole (Fig. S3). We considered whether iHA-*Tg*ATP4 knockdown resulted in decreased viability of extracellular parasites, as has been observed in mutants of a gene involved in *T. gondii* stress responses (30). Parasites were grown in the absence or presence of ATc for 2 days, mechanically released from host cells by passage through a 26-gauge needle, and incubated in standard growth medium (which has a high $[Na^+]$) for 0–27 h. Parasites were then labeled for 20 min in propidium iodide (a membrane-impermeant DNA dye frequently used to assess cell viability; 31) and analyzed by flow cytometry. In all cases, parasite viability declined over the 27-h incubation; however, the viability of iHA-*Tg*ATP4 parasites grown in the presence of ATc decreased more rapidly than that of iHA-*Tg*ATP4 parasites grown in the absence of ATc or of WT controls, with statistical significance reached after a 20-h incubation in the growth medium (Fig. 3*D*; $n = 4$, $p \leq 0.003$, one-way ANOVA). In summary, *Tg*ATP4 is important for the growth of *T. gondii* parasites over multiple lytic cycles and is not required for intracellular growth, egress or invasion but is important for maintaining the viability of extracellular parasites.

TgATP4-disrupted parasites show reduced virulence in mice

To investigate the impact of *Tg*ATP4 on parasite virulence *in vivo*, we generated parasites in which the ORF of *Tg*ATP4 was disrupted using CRISPR-Cas9 targeted genome editing. We designed a single guide RNA (gRNA) that targeted the first exon of the *Tg*ATP4 ORF (Fig. S4*A*) and transfected this into WT RHΔhxgprt/Tomato parasites (32). We identified a clonal parasite strain with a 113-bp insertion in the *Tg*ATP4 locus, resulting in incorporation of a premature stop codon in the *Tg*ATP4

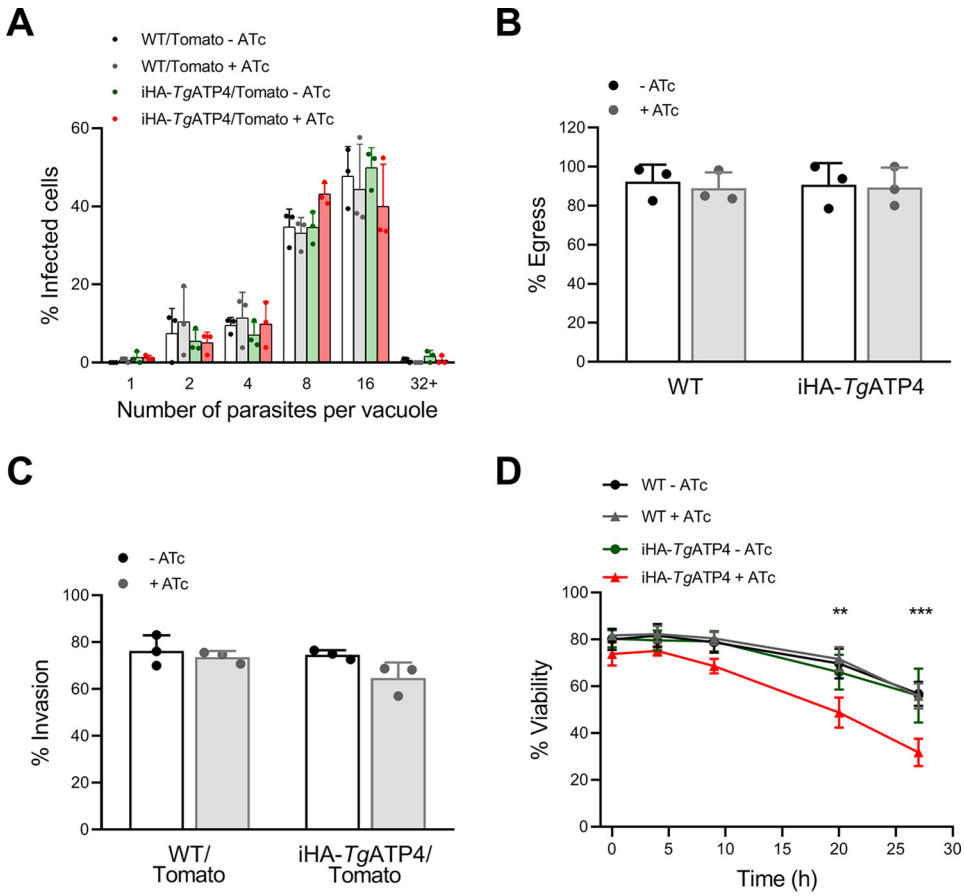

Figure 3. Investigation of the importance of *Tg*ATP4 for intracellular growth, egress, and invasion. *A*, to measure intracellular parasite growth, WT/Tomato and iHA-*Tg*ATP4/Tomato parasites were grown in the presence and absence of ATc for 2 days. Parasites were allowed to invade host cells and then cultured for 24 h before fixing the cells and counting the number of parasites per vacuole. *B*, the ability of WT and iHA-*Tg*ATP4 parasites (maintained for 30 h in the presence or absence of ATc) to egress from their host cells after a 3-min exposure to the Ca^{2+} ionophore A23187 (2 μM). *C*, WT/Tomato and iHA-*Tg*ATP4/Tomato parasites were grown in the absence and presence of ATc for 2 days and then allowed to invade host cells for 10 min. *D*, to measure extracellular parasite viability, WT and iHA-*Tg*ATP4 parasites were grown in the absence or presence of ATc for 2 days. Intracellular parasites were then mechanically egressed from host cells and incubated as extracellular parasites in (high-[Na^+]) growth medium for 0–27 h. The viability of parasites was monitored at predetermined time points by labeling with propidium iodide. In *A–C*, the *bars* show the mean values (with the *error bars* showing S.D.) averaged from three independent experiments. The data from individual experiments are shown with *circles*. In *D*, the data shown are the mean values (± S.D.) averaged from four independent experiments (*asterisks* denote statistically significant differences between iHA-*Tg*ATP4 parasites incubated in the presence of ATc and all other parasites and conditions: **, $p < 0.01$; ***, $p < 0.001$; one-way ANOVA). Where not shown, *error bars* fall within the symbols.

ORF (Fig. S4*B*). This strain will synthesize a truncated, and likely nonfunctional, *Tg*ATP4 protein that lacks residues 34 to 1338. We termed this strain *atp4*$^{\Delta 34-1338}$. Plaque assays revealed that *atp4*$^{\Delta 34-1338}$ parasites exhibited a growth defect *in vitro* (Fig. S4*C*). Complementation of *atp4*$^{\Delta 34-1338}$ parasites with a constitutively expressed copy of *Tg*ATP4 (yielding the strain "*atp4*$^{\Delta 34-1338}$/cTy1-*Tg*ATP4") rescued the *in vitro* growth phenotype (Fig. S4*C*).

To determine whether *Tg*ATP4 influences parasite virulence *in vivo*, we infected mice with either WT, *atp4*$^{\Delta 34-1338}$, or *atp4*$^{\Delta 34-1338}$/cTy1-*Tg*ATP4 parasites. In each case, five BALB/c mice were infected intraperitoneally with 10^3 parasites. All mice infected with WT or *atp4*$^{\Delta 34-1338}$/cTy1-*Tg*ATP4 parasites exhibited symptoms of toxoplasmosis and were euthanized on Day 6 or 7 post-infection (Fig. 4). In contrast, mice infected with *atp4*$^{\Delta 34-1338}$ parasites did not display disease symptoms until Day 9 or 10 post-infection (Fig. 4). Thus, parasites lacking *Tg*ATP4 can cause disease *in vivo*, but their virulence is reduced.

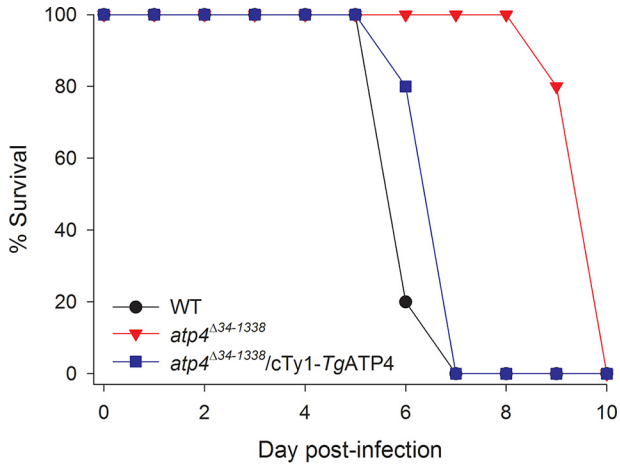

Figure 4. Virulence of *Tg*ATP4-expressing and *TgATP4*-disrupted parasites in mice. Five BALB/c mice were infected with 10^3 WT (*black*), *atp4*$^{\Delta 34-1338}$ (*red*), or *atp4*$^{\Delta 34-1338}$/cTy1-*Tg*ATP4 (*blue*) parasites and monitored for progression of disease. The data are from a single experiment.

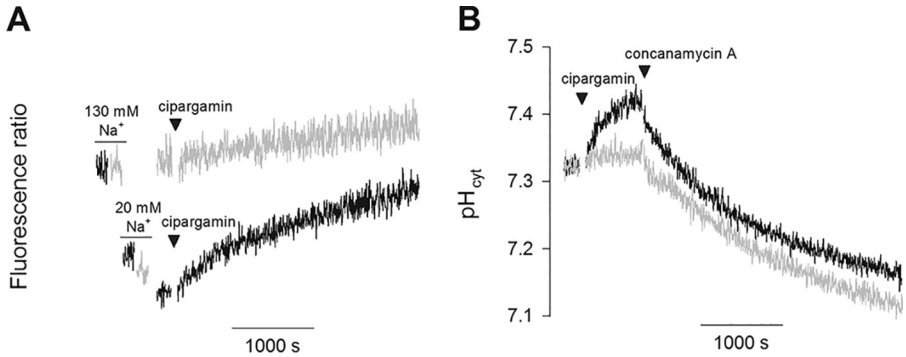

Figure 5. Na^+ and pH regulation in *Tg*ATP4-expressing and *Tg*ATP4 knockdown parasites and the effect of cipargamin thereon. *A* and *B*, representative traces showing the effects of cipargamin on $[Na^+]_{cyt}$ (*A*) and pH_{cyt} (*B*) in iHA-*Tg*ATP4 parasites expressing *Tg*ATP4 (−*ATc*, *black*) and in parasites in which *Tg*ATP4 is knocked down (+*ATc*, *gray*). Each trace is representative of at least three similar experiments. Parasites were suspended in physiological saline, and the concentration of cipargamin added was 50 nM. Calibration traces for 20 mM and 130 mM Na^+ are depicted to the *left* of the main traces. In *B*, concanamycin A was added at a concentration of 100 nM to inhibit the plasma membrane V-type H^+-ATPase.

TgATP4 is important for Na^+ regulation in T. gondii

The addition of antimalarial spiroindolones or other compounds believed to inhibit *Pf*ATP4 to isolated *P. falciparum* parasites results in an immediate-onset, gradual increase in both $[Na^+]_{cyt}$ and pH_{cyt} (10, 12–16, 18) but no change in $[Ca^{2+}]_{cyt}$ (10, 15). We investigated the role of *Tg*ATP4 in regulating $[Na^+]_{cyt}$, pH_{cyt}, and $[Ca^{2+}]_{cyt}$ in *T. gondii* using the Na^+-sensitive fluorescent indicator SBFI, the pH-sensitive fluorescent indicator BCECF, and the Ca^{2+}-sensitive fluorescent indicator Fura-2, respectively. In each case, cultures containing iHA-*Tg*ATP4 parasites were exposed to either ATc or 0.025% (v/v) ethanol (solvent control) for 2 days leading up to the experiment. On the day of the experiment, the appropriate fluorescent indicator was loaded into *T. gondii* tachyzoites that had either recently emerged from their host cells or that had been released from their host cells by passage of the culture through a 26-gauge needle. The dyes are all ratiometric, and an increase in the measured fluorescence ratio corresponds to an increase in $[Na^+]_{cyt}$ (SBFI), pH_{cyt} (BCECF), or $[Ca^{2+}]_{cyt}$ (Fura-2).

We incubated iHA-*Tg*ATP4 parasites grown in the absence of ATc (*i.e.* expressing *Tg*ATP4) in a saline solution containing 130 mM Na^+ and measured the resting $[Na^+]_{cyt}$. We found that the resting $[Na^+]_{cyt}$ was less than 20 mM (Fig. 5*A*). Upon addition of cipargamin (50 nM; a concentration that has been used in similar experiments with isolated *P. falciparum* parasites (16)), the $[Na^+]_{cyt}$ in these parasites increased (Fig. 5*A*). The cipargamin-induced increase in Na^+ content in *T. gondii* parasites was confirmed using an alternate, HPLC-based approach (Fig. S5). In contrast, in iHA-*Tg*ATP4 parasites that had been exposed to ATc for 2 days to knock down *Tg*ATP4 expression, the resting $[Na^+]_{cyt}$ was ~130 mM (*i.e.* close to the $[Na^+]$ in the medium in which the parasites were suspended; Fig. 5*A*). Cipargamin had little effect on $[Na^+]_{cyt}$ in these parasites (Fig. 5*A*). These data indicate that, as proposed for *Pf*ATP4, *Tg*ATP4 plays a key role in maintaining a low $[Na^+]_{cyt}$ in the parasite. Our data are consistent with *Tg*ATP4 functioning as an Na^+ efflux pump and being inhibited by nanomolar concentrations of cipargamin.

We next measured the effects of cipargamin and *Tg*ATP4 knockdown on resting pH_{cyt}. We found that the resting pH_{cyt} of iHA-*Tg*ATP4 parasites grown in the absence or presence of ATc was similar (7.33 ± 0.09 and 7.40 ± 0.08, respectively; $p = 0.10$, unpaired *t* test; mean ± S.D.; $n = 8$). However, iHA-*Tg*ATP4 parasites expressing *Tg*ATP4 (−ATc), but not those with *Tg*ATP4 knocked down (+ATc), were found to undergo a cytosolic alkalinization upon addition of 50 nM cipargamin (Fig. 5*B*). This is consistent with the hypothesis that *Tg*ATP4 extrudes Na^+ in exchange for H^+, maintaining a low $[Na^+]_{cyt}$ while at the same time imposing an acid load on the parasite. Inhibition of *Tg*ATP4 results in a lifting of this load and consequent cytosolic alkalinization.

The V-type H^+-ATPase inhibitor concanamycin A (100 nM) resulted in a cytosolic acidification in parasites that had been maintained both with (+) or without (−) ATc (Fig. 5*B*). This is consistent with previous evidence that the V-type H^+-ATPase plays a key role in pH regulation in *T. gondii* (6) and, importantly, shows that the parasites that had been maintained in the presence of ATc for 2 days were still actively maintaining their resting pH (and, hence, were metabolically active) at the time point at which all of our fluorometric assays were performed.

The spiroindolone cipargamin is one of a structurally diverse range of antimalarial agents that inhibit *P. falciparum* growth through an effect on ion homeostasis, attributed to inhibition of Na^+ efflux via *Pf*ATP4 (10, 13–16). The pyrazoleamide PA21A050 is another such compound, structurally unrelated to the spiroindolones (15). To determine whether PA21A050 can inhibit *T. gondii* growth, we performed fluorescence growth assays. The growth of *T. gondii* parasites was inhibited by PA21A050 with an IC_{50} of 0.56 ± 0.17 μM (mean ± S.D.; $n = 3$; Fig. 6*A*). This IC_{50} value is much higher than the previously reported IC_{50} value for inhibition by PA21A050 of the proliferation of blood-stage *P. falciparum* parasites (~0.7 nM (15)). We investigated whether PA21A050, like cipargamin, impaired Na^+ homeostasis in *T. gondii*. As seen for cipargamin, addition of PA21A050 (50 nM) to iHA-*Tg*ATP4 parasites grown in the absence of ATc resulted in an increase in $[Na^+]_{cyt}$ (Fig. 6*B*). Addition of PA21A050 to iHA-*Tg*ATP4 parasites grown in the presence of ATc had little effect on the (already high) $[Na^+]_{cyt}$ (Fig. 6*B*).

We next measured the effects of PA21A050 on resting pH_{cyt}. Again, as seen for cipargamin, addition of PA21A050 to iHA-

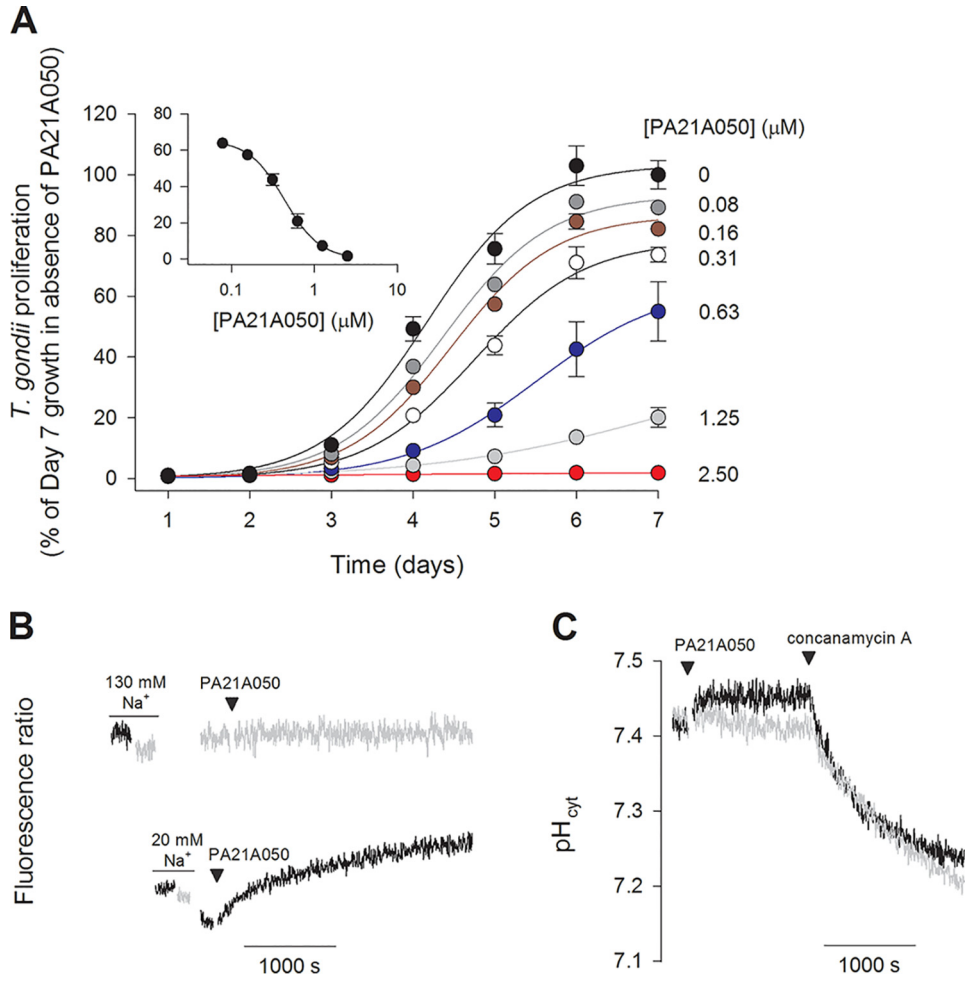

Figure 6. The effect of the pyrazoleamide PA21A050 on *T. gondii* growth, $[Na^+]_{cyt}$, and pH_{cyt}. *A*, the effect of various concentrations of the pyrazoleamide PA21A050 on the growth of WT/Tomato parasites over the course of 7 days. The data shown are from a single experiment (with *error bars* showing the standard deviation of triplicate measurements) and are representative of those obtained in three independent experiments. For clarity, the data points for 5 μM and 10 μM PA21A050 are not shown (they overlapped with those for 2.5 μM PA21A050). *Inset*, the data for Day 5 shown in the main panel are plotted against the concentration of PA21A050 to generate a dose–response curve. Where not shown, *error bars* fall within the symbols. *B* and *C*, representative traces showing the effects of PA21A050 on $[Na^+]_{cyt}$ (*B*) and pH_{cyt} (*C*) in iHA-*Tg*ATP4 parasites expressing *Tg*ATP4 (−*ATc*, *black*) and in parasites in which *Tg*ATP4 is knocked down (+*ATc*, *gray*). Each trace is representative of at least three similar experiments. Calibration traces for 20 mM and 130 mM Na^+ are depicted to the *left* of the main traces. Parasites were suspended in physiological saline, and PA21A050 was added at a concentration of 50 nM. Concanamycin A (*C*) was added at a concentration of 100 nM to inhibit the V-type H^+-ATPase.

*Tg*ATP4 parasites grown in the absence of ATc resulted in an increase in resting pH_{cyt} (Fig. 6*C*). No such increase was observed in iHA-*Tg*ATP4 parasites grown in the presence of ATc (Fig. 6*C*). The pyrazoleamide PA21A050 therefore affects Na^+ and pH homeostasis in a manner similar to cipargamin.

TgATP4 does not play a direct role in Ca^{2+} regulation in T. gondii

We next examined the role of *Tg*ATP4 in Ca^{2+} regulation using the Ca^{2+}-sensitive dye Fura-2. The resting cytosolic $[Ca^{2+}]$ ($[Ca^{2+}]_{cyt}$) was similar in *Tg*ATP4-expressing and *Tg*ATP4 knockdown parasites (Fig. 7*A*), and addition of cipargamin had little effect on $[Ca^{2+}]_{cyt}$ in either case (Fig. 7*A*). We also compared the ability of *Tg*ATP4-expressing and *Tg*ATP4 knockdown parasites to regulate their $[Ca^{2+}]_{cyt}$ in the presence of increasing external $[Ca^{2+}]$. *Tg*ATP4-expressing and *Tg*ATP4 knockdown parasites were both able to regulate their $[Ca^{2+}]_{cyt}$, with $[Ca^{2+}]_{cyt}$ maintained at less than 150 nM in the presence of external $[Ca^{2+}]$ of up to 1 mM (the highest concentration tested; Fig. 7*B*) for both strains and with no discernible difference between them ($p > 0.39$, unpaired *t* tests). Decreased expression of *Tg*ATP4 therefore has no significant effect on Ca^{2+} regulation in these parasites.

Discussion

The first sequence analyses of *Pf*ATP4 led to annotation of this protein as a Ca^{2+} transporter (8, 33, 34), albeit one that was phylogenetically distinct from other types of Ca^{2+} ATPases that had been categorized at that time. These studies also identified residues in *Pf*ATP4 that were proposed to be involved in Ca^{2+} binding (8, 33, 34). In a detailed phylogenetic analysis of the 265-residue core region of 159 P-type ATPases, Axelsen and Palmgren (24) placed *Pf*ATP4 in the type IIA subgroup of P-type ATPases, most members of which are believed to transport Ca^{2+}. However, few organisms belonging to the Apicomplexa or closely related phyla were included in their analysis. It has also been suggested that *Pf*ATP4 might be an ENA (a type IID P-type ATPase) (10). This suggestion was based on an

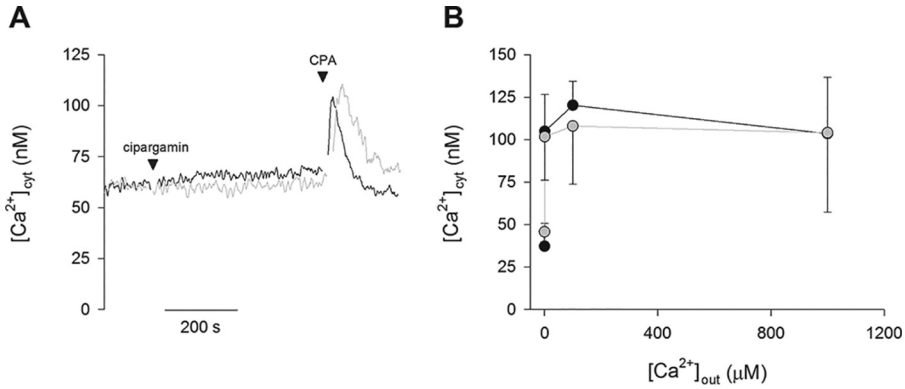

Figure 7. Ca^{2+} regulation in *Tg*ATP4-expressing and *Tg*ATP4 knockdown parasites and the effect of cipargamin. *A*, traces showing the effects of cipargamin on $[Ca^{2+}]_{cyt}$ in iHA-*Tg*ATP4 parasites expressing *Tg*ATP4 (−*ATc*, *black*) and in parasites in which *Tg*ATP4 is knocked down (+*ATc*, *gray*). The traces are representative of those obtained in at least three similar experiments for each condition. The parasites were suspended in physiological saline, and the concentration of cipargamin was 50 nM. Cyclopiazonic acid (*CPA*) was added at a concentration of 10 μM to release the endoplasmic reticulum Ca^{2+} store (59) and confirm that the assay enabled the detection of changes in $[Ca^{2+}]_{cyt}$. *B*, the $[Ca^{2+}]_{cyt}$ in iHA-*Tg*ATP4 parasites expressing *Tg*ATP4 (−*ATc*, *black symbols*) and in parasites in which *Tg*ATP4 was knocked down (+*ATc*, *gray symbols*) in the presence of varying external $[Ca^{2+}]$ ($[Ca^{2+}]_{out}$). The data are averaged from those obtained in four independent experiments performed on different days and are shown as the mean ± S.D. The $[Ca^{2+}]_{cyt}$ values for *Tg*ATP4-expressing and *Tg*ATP4 knockdown parasites were compared at each $[Ca^{2+}]_{out}$ using unpaired *t* tests. There was no significant difference between the $[Ca^{2+}]_{cyt}$ in the two strains at any of the $[Ca^{2+}]_{out}$ values tested.

eight-residue sequence in *Pf*ATP4 (^{849}IVQSLKRK) with similarity to a semiconserved motif in ENA ATPases (MIEALHRR in ScENA1). Included in this motif is a triplet of positively charged residues (KRK in *Pf*ATP4) that may be important for Na^+ transport (35). However, our analysis using the entire P-type ATPase core sequence and a dataset containing representatives from a variety of organisms, including members of the Apicomplexa, Dinoflagellata, and Chromerida, reveal that ATP4 proteins do not belong to one of the previously defined subgroups of P-type ATPases but, rather, represent a distinct subgroup. One consequence of this is that the function or substrate specificity of the ATP4 proteins cannot be inferred from their sequences and must be determined experimentally.

In this study, we found that cipargamin and PA21A050 induced a gradual, immediate-onset increase in both $[Na^+]_{cyt}$ and pH_{cyt} in *T. gondii* parasites expressing *Tg*ATP4. This mirrors the results of equivalent experiments in *P. falciparum* (10, 15). Notably, we observed no increases in $[Na^+]_{cyt}$ and pH_{cyt} in parasites in which *Tg*ATP4 was knocked down. Unlike *Tg*ATP4-expressing parasites, which maintained a low $[Na^+]_{cyt}$ of less than 20 mM in a solution with a high $[Na^+]$ similar to that found in serum and extracellular fluid (130 mM), *Tg*ATP4 knockdown parasites were unable to regulate their $[Na^+]_{cyt}$ and had an internal $[Na^+]$ similar to that of the extracellular solution. Together, these data are consistent with ATP4 function being conserved between *P. falciparum* and *T. gondii* and provide genetic evidence that ATP4 proteins are cipargamin- and PA21A050-sensitive pumps that extrude Na^+ while importing H^+. However, the possibility that the flux of H^+ equivalents that accompanies the transport of Na^+ does not occur directly via ATP4 cannot be excluded.

Extracellular parasites lacking *Tg*ATP4 lost viability more rapidly than parasites expressing *Tg*ATP4. Upon prolonged extracellular incubation (~ 6–12 h), these parasites appeared swollen and frequently contained a large internal vacuole that resembled the previously described plant-like vacuole of the parasite (36). The plant-like vacuole has been associated with parasite tolerance to salt stress (36), and its apparent increase in size in extracellular parasites lacking *Tg*ATP4 may represent a parasite response to the presence of high $[Na^+]_{cyt}$. Our observation that extracellular *T. gondii* parasites swell upon depletion of *Tg*ATP4 is in line with previous studies reporting that *P. falciparum* parasites swell on exposure to compounds believed to inhibit *Pf*ATP4 (9, 13, 15, 16). The observation that the pH_{cyt} of *Tg*ATP4-knockdown parasites was not significantly different from that of *Tg*ATP4-expressing parasites indicates that although, when present, *Tg*ATP4 imposes a significant acid load on the parasite, it does not play a major role in maintaining the normal resting pH_{cyt}.

In the first experimental investigation of ATP4 function, it was reported that membranes prepared from *Xenopus* oocytes that had been injected with *PfATP4* cRNA displayed greater Ca^{2+}-ATPase activity than membranes from noninjected oocytes (8). Others have since reported being unable to reproduce these findings (7, 37). Furthermore, addition to isolated *P. falciparum* parasites of either the spiroindolone NITD246 (10) or the pyrazoleamide PA21A050 (15) (for which resistance is mediated by mutation of *Pf*ATP4 (7, 15)) resulted in an increase in $[Na^+]_{cyt}$ and pH_{cyt} but no change in $[Ca^{2+}]_{cyt}$ (10, 15). Consistent with this, Ca^{2+} did not stimulate the cipargamin-sensitive ATPase activity measured in *P. falciparum* membrane preparations (17). Our observations that cipargamin had no significant effect on $[Ca^{2+}]_{cyt}$ in *T. gondii* and that *Tg*ATP4 knockdown parasites were no less effective than *Tg*ATP4-expressing parasites in regulating their $[Ca^{2+}]_{cyt}$ in the face of increasing external $[Ca^{2+}]$ provide further evidence against a role for ATP4 in parasite Ca^{2+} regulation. Our findings that extracellular *Tg*ATP4 knockdown parasites cannot maintain their plasma membrane Na^+ gradient but maintain tight control over their $[Ca^{2+}]_{cyt}$ suggest that the parasite is not reliant on a plasma membrane Na^+/Ca^{2+} exchanger to regulate $[Ca^{2+}]_{cyt}$. Orthologs of Na^+/Ca^{2+} exchanger genes are lacking in apicomplexan parasites, and to the extent of our knowledge, there is no evidence, either from genomic or physiological data, that *T. gondii* parasites possess a Na^+/Ca^{2+} exchange system. We conclude that *Tg*ATP4 is required for Na^+ regulation but

not for maintaining the normal cytosolic pH or Ca^{2+} concentration in *T. gondii* parasites.

Although a 50 nM concentration of either the spiroindolone cipargamin or the pyrazoleamide PA21A050 was sufficient to perturb pH_{cyt} and $[Na^+]_{cyt}$ in extracellular tachyzoites (Figs. 5 and 6), much higher concentrations of each of these compounds were needed to inhibit the proliferation of the parasite. An IC_{50} of 1 μM has been reported for inhibition of the proliferation of *T. gondii* tachyzoites by cipargamin (23); for *P. falciparum*, the IC_{50} is orders of magnitude lower (~ 1 nM (7)). Similarly, our testing of PA21A050, a structurally unrelated *Pf*ATP4 inhibitor, for its effect on the proliferation of *T. gondii* revealed an IC_{50} value more than 500-fold higher than that reported for *P. falciparum* (15). Other antiplasmodial compounds that are believed to inhibit *Pf*ATP4 (*Pf*ATP4-associated compounds) also lack potency against *T. gondii*. Of the 28 antiplasmodial *Pf*ATP4-associated compounds identified in the 400-compound "Malaria Box" (14), all lacked potency against *T. gondii* growth, with IC_{50} values greater than 14 μM in all cases (38). Thus, the available data indicate that, whereas in *P. falciparum* cipargamin and PA21A050 both perturb ion homeostasis and inhibit parasite proliferation in the nanomolar range, in *T. gondii* the concentrations required to inhibit parasite proliferation are much higher than those required to perturb ion homeostasis. Given that parasites can continue to proliferate (albeit at a reduced rate) in the absence of *Tg*ATP4 expression, it is likely that cipargamin and PA21A050 exert their growth-inhibitory effects on *T. gondii* via targets other than *Tg*ATP4.

The differential susceptibility of *P. falciparum* and *T. gondii* to growth inhibition by ATP4 inhibitors might be explained on the basis of the different ionic conditions each of the two parasites experience in the course of their asexual cycles. Both cells spend the majority of their asexual lytic cycles within host cells; for *T. gondii*, these can be nucleated cells of any type, whereas for *P. falciparum* (during the disease-causing stage of malaria), the host cells are erythrocytes. Mammalian cells maintain a low resting $[Na^+]_{cyt}$. In the case of *T. gondii*-infected cells, there is no evidence of significant perturbation of host cell ion homeostasis; it is therefore presumed that the intracellular *T. gondii* parasite is exposed to a low-$[Na^+]$ environment, and the parasite itself may therefore have little if any need to expend energy on extruding Na^+ ions, relying instead on the host cell's homeostatic mechanisms (Fig. 8). This might explain our finding that the intracellular growth of *T. gondii* is not affected when *Tg*ATP4 is knocked down. By contrast, while inside a human erythrocyte, the asexual-stage *P. falciparum* parasite induces profound changes to the permeability of the host erythrocyte membrane, through so-called new permeability pathways, such that the membrane can no longer maintain a large Na^+ gradient, and $[Na^+]_{cyt}$ is increased to levels comparable with that in the extracellular medium (Fig. 8) (39–42). Consequently, the *P. falciparum* parasite is exposed to a high-$[Na^+]$ environment for much of its 48 h occupancy of the erythrocyte (from ~ 20 h to 48 h post-invasion) (39). This might be expected to render *P. falciparum* dependent on its Na^+ extrusion mechanism for most of its intraerythrocytic cycle, and hence particularly vulnerable to ATP4 inhibition (Fig. 8).

Knockdown and disruption of *Tg*ATP4 impaired, but did not fully inhibit, *T. gondii* proliferation (Fig. 2*D*) (Fig. S4). We also observed a defect in parasite virulence upon *Tg*ATP4 disruption (Fig. 4). A recent genome-wide CRISPR-based screen provided evidence that *Tg*ATP4 is important for normal *T. gondii* growth, with *Tg*ATP4 ranked in the top 7% of the most important genes in the parasite ("phenotype score" of −4.77 (43)). The growth and virulence defects we observed were perhaps less pronounced than what may have been expected from the genome-wide study. We observed no significant decreases in invasion, intracellular growth, or egress upon *Tg*ATP4 knockdown (Fig. 3, *A–C*), consistent with the growth defect being due to an effect of *Tg*ATP4 knockdown on the parasite at another part of the lytic cycle. The inability of *Tg*ATP4 knockdown parasites to regulate $[Na^+]_{cyt}$ is likely to make these parasites particularly sensitive to high-$[Na^+]$ conditions, as prevail in the extracellular medium (Fig. 8). Consistent with this, we found that the decline in the viability of extracellular parasites over time was more rapid for *Tg*ATP4 knockdown parasites than for parasites expressing *Tg*ATP4 (Fig. 3*D*). We conclude that *Tg*ATP4 is of particular importance in the extracellular stage of the *T. gondii* lytic cycle, consistent with its proposed role in mediating Na^+ homeostasis in the parasite (Fig. 8).

In summary, this study provides genetic evidence that the *T. gondii* ATP4 protein, *Tg*ATP4, plays an important role in the extracellular stage of the lytic cycle of this parasite and functions as a spiroindolone- and pyrazoleamide-sensitive Na^+/H^+ pump, acting to extrude Na^+ from the parasite and maintain a low $[Na^+]_{cyt}$. The *Tg*ATP4 knockdown and disrupted lines provide tools for future functional studies to elucidate the importance of key residues in the ATP4 protein. For example, complementing the inducible *Tg*ATP4 knockdown line described here with mutant versions of *Tg*ATP4 (or with ATP4 variants from other organisms) will enable the roles of individual ATP4 residues, both in the function of the protein and in conferring resistance to *Pf*ATP4 antagonists, to be established.

Although Na^+-regulation in *T. gondii* and *P. falciparum* parasites is sensitive to nanomolar concentrations of ATP4 inhibitors, our results suggest key differences in the effects of ATP4 inhibition on the growth of the two parasite species. These differences may be accounted for by the different exposure to extracellular Na^+ experienced by the two parasites. *P. falciparum* parasites are exposed to high external Na^+ levels throughout much of the intracellular phase of their intraerythrocytic cycle, whereas exposure of *T. gondii* parasites to a high external Na^+ level is largely restricted to the extracellular phase of their lytic cycle. Together with the observation that parasites lacking *Tg*ATP4 have only a slight reduction in virulence, these findings raise important reservations about the utility of *Tg*ATP4 as a drug target in *T. gondii*.

Finally, our phylogenetic analysis indicates that ATP4 proteins constitute a distinct subgroup within the type II P-type ATPases, although proof that *Tg*ATP4 has a P-type ATPase mechanism requires additional study. Nevertheless, our data are consistent with ATP4-type ATPases having conserved roles as ATP-dependent Na^+ pumps in apicomplexans and their relatives. The last common ancestors of apicomplexans, chromerids, and dinoflagellates were free-living organisms that inhab-

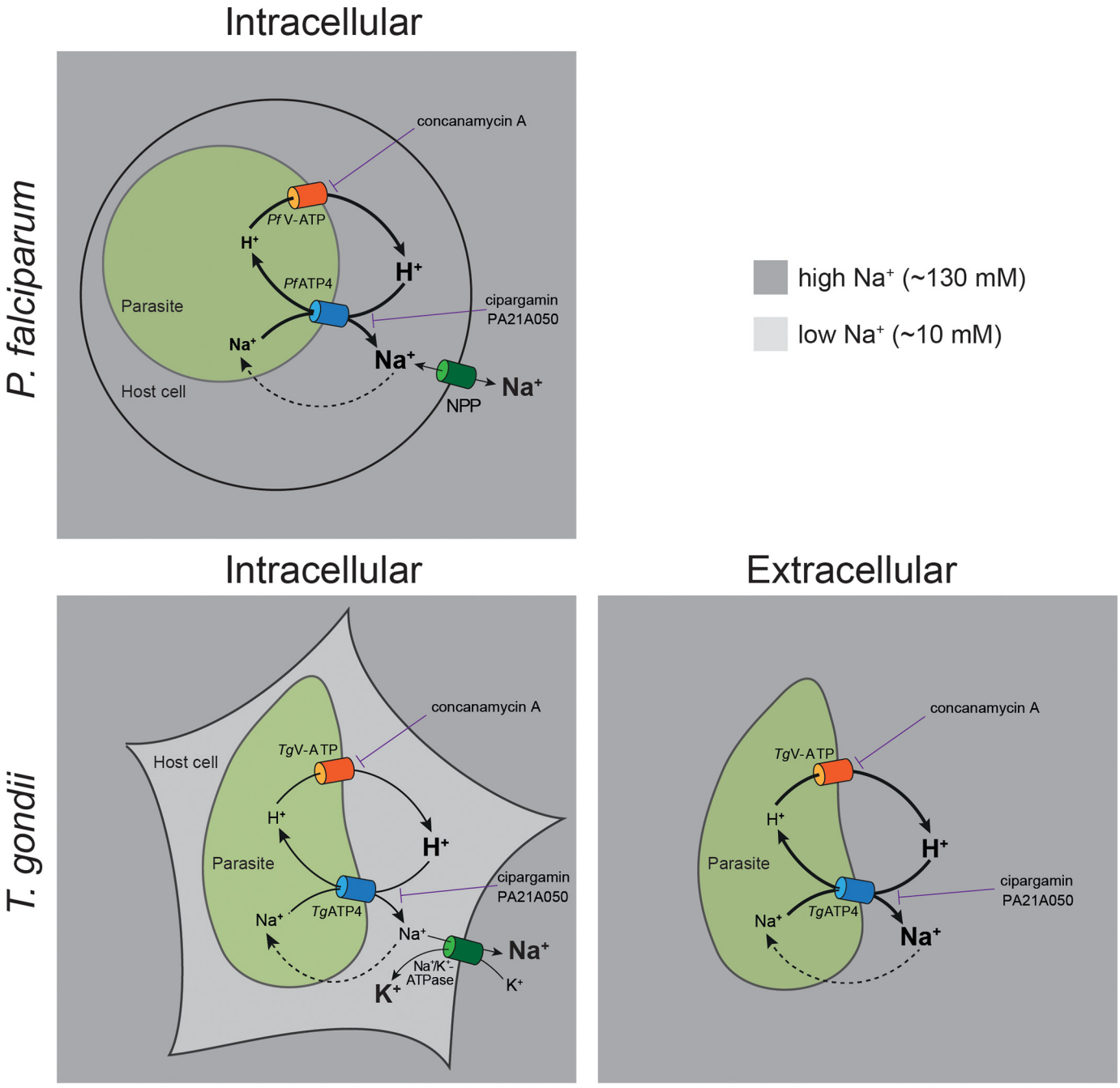

Figure 8. Schematic illustrating how differences in the lifestyles of *P. falciparum* and *T. gondii* might explain their different sensitivities to ATP4 inhibitors. *P. falciparum* trophozoites modify erythrocytes by inducing new permeability pathways (*NPP*) that mediate the net influx of Na^+ across the erythrocyte plasma membrane, exposing the intracellular parasite to a high external [Na^+] (~130 mM). Uncharacterized "leak pathways" (represented by a *dotted line*) mediate the influx of Na^+ from the host cytosol into the parasite. The cipargamin- and PA21A050-sensitive ATP4 pump extrudes Na^+ ions, maintaining a low [Na^+] inside the parasite. The pump is proposed to import H^+ as it exports Na^+, with the imported H^+ being extruded from the parasite by the concanamycin A–sensitive V-type H^+-ATPase (*V-ATP*) (10). *T. gondii* tachyzoites reside in host cells that maintain a low-[Na^+] environment ([Na^+] ~10 mM) through the action of the host plasma membrane Na^+/K^+-ATPase. Under these (low-intracellular-[Na^+]) conditions, the parasite is not reliant on its own Na^+ regulation mechanisms to maintain a low $[Na^+]_{cyt}$. However, upon egress from their host cells, extracellular tachyzoites are exposed to the high-[Na^+] extracellular medium ([Na^+] ~130 mM) and must actively extrude Na^+ via ATP4 to maintain a low $[Na^+]_{cyt}$.

ited a marine environment (44), and it is conceivable that ATP4-type ATPases first evolved a role in regulating $[Na^+]_{cyt}$ in the high-Na^+ (~ 460 mM (45)) marine environment.

Experimental procedures

Ethics statement

Mouse studies examining *T. gondii* virulence were performed according to procedures outlined in protocol A2016/42, approved by the Australian National University Animal Experimentation Ethics Committee.

Phylogenetic analysis of TgATP4

*Tg*ATP4 homologs and a representative selection of type II P-type ATPases from a broad range of eukaryotic organisms were aligned using ClustalX (46). The accession numbers for the proteins in the dataset are in shown in Fig. 1. The "acces-

sion.version" sequence identifiers are provided for sequences that are in the NCBI database. *S. minutum* accession numbers were derived from the *S. minutum* genome browser (http://marinegenomics.oist.jp/)[7] (47). The *Hematodinium* sequences are available in BioProject PRJNA317731 (48), and the *C. velia* sequence CveI-6710 is available through the Uniprot database. The editing software Jalview was used to trim the alignment to the core sequence of 265 residues for P-type ATPases as defined by Axelsen and Palmgren (24). The dataset was subjected to maximum likelihood phylogenetic analysis using PHYLIP as described previously (49). Bootstrap analysis, which provides a statistical measure of confidence in the nodes of the phylogenetic tree, was performed using 1000 replicates.

Host cell and parasite culture

T. gondii was cultured in human foreskin fibroblasts (a kind gift from Holger Schlüter, Peter MacCallum Cancer Centre) in DMEM supplemented with 1% (v/v) fetal calf serum, 200 μM L-glutamine, 50 units/ml penicillin, 50 μg/ml streptomycin, 10 μg/ml gentamicin, and 0.25 μg/ml amphotericin B. Cells were cultured at 37 °C in a humidified 5% CO_2 incubator. Unless stated otherwise, the type I TATi/Δ*ku80* strain was used as the parental strain for the parasites generated in this study (50). Where applicable, ATc (dissolved in ethanol) was added at a final concentration of 0.5 μg/ml, yielding a final ethanol concentration of 0.025% (v/v).

Generation of genetically modified T. gondii lines

To generate a 3′ HA tag replacement in the *TgATP4* locus, we amplified the 3′ region of the *TgATP4* ORF using the primers 5′-GACTGGATCCGACCCACATCGATTTTTGGAATCC and 5′-CATGCCTAGGGGCCATAATCGCCGGCGCTTTGGAAG. We digested the resultant product with BamHI and AvrII and ligated this into the BglII and AvrII sites of the vector pgCH (32). This vector was linearized with BglII, transfected into TATi/Δ*ku80* strain parasites, and selected on chloramphenicol as described previously (51). To generate the *Tg*ATP4 knockdown parasite strain, we first amplified a 3′ flank region of the *TgATP4* locus with the primers 5′-GATCACCGGTATGGCGGCCCGAGCATCG and 5′-GACTGCGGCCGCGAGAGGAGTTTTTCAACACATCGGC. We digested the PCR product with AgeI and NotI and ligated this into the XmaI and NotI sites of the vector pPR2-HA_3 (52). We then amplified a 5′ flank region of the *TgATP4* locus with the primers 5′-TGACGGGCCCCTGCTACAAGCGAGTCTATGGTGGC and 5′-GCATTTAATTAAGCTAGTGGATGCGTGGAGAAAGTCG. We digested this product with ApaI and PacI and ligated this into the equivalent sites of the pPR2-HA_3 vector already harboring the 3′ flank. We digested the resultant vector with NotI, transfected into TATi/Δ*ku80* strain parasites, and selected on pyrimethamine as described previously (51). This generated the strain we termed iHA-*Tg*ATP4. To verify successful integration of the iHA-*Tg*ATP4 construct into the *TgATP4* locus, we performed PCR screens with the primers "screen fwd" (5′-AATCGCATCCTCGGATCTTG) and "screen rvs" (5′-AAGAGACGTGCTTCGCAGAG) to detect the presence of the native locus and the primers "t7s4 fwd" (5′-ACGCAGTTCTGCCAAGACG) and screen rvs to detect the presence of the modified locus. To enable us to perform fluorescence growth assays, we introduced a tandem dimeric Tomato red fluorescent protein into the iHA-*Tg*ATP4 strain as described previously (32). To complement the iHA-*Tg*ATP4 strain with a constitutively expressed *TgATP4*, we synthesized the *TgATP4* gene (Sigma-Aldrich). The synthesized gene harbored a 5′ XmaI and a 3′ PstI site. We digested the synthesized gene with XmaI and PstI and ligated this into the equivalent sites of the vector pUgCTTy (53), which places the *TgATP4* gene downstream of the α-tubulin promoter, and fused with an N-terminal 5×Ty1 epitope tag (generating a vector we termed pUgCTTy(*TgATP4*)). We linearized this vector with MfeI, transfected into iHA-*Tg*ATP4 parasites, and selected on chloramphenicol. All parasite strains were cloned by limiting dilution before characterization.

To generate a parasite strain in which the *TgATP4* ORF was disrupted, we adopted a CRISPR/Cas9-based genome editing approach. Using Q5 site-directed mutagenesis (New England Biolabs), we modified the pSAG::Cas9-U6::sgUPRT vector (Addgene plasmid 54467 (54)) to express a gRNA targeting the first exon of the *TgATP4* ORF. We PCR-amplified this vector using the primers 5′-ACTTCCTCGAGCGCAGACGGGTTTTAGAGCTAGAAATAGCAAG (the underlined sequence encodes the *TgATP4* targeting region) and 5′-AACTTGACATCCCCATTTAC and circularized the PCR product according to the manufacturer's instructions (New England Biolabs). The resultant vector co-expresses the *TgATP4*-targeting gRNA and Cas9-GFP. We transfected this vector into type I RH/Δhxgprt/Tomato strain parasites (32) and cloned GFP-positive parasites 3 days after transfection. A mutant clone containing a frameshift mutation (a 113-bp insertion) was identified and further verified by direct Sanger sequencing of the *TgATP4* locus. The resultant strain, termed $atp4^{\Delta 34-1338}$, was complemented by integration of the pUgCTTy(*TgATP4*) vector as described above.

Immunofluorescence assays and Western blotting

Immunofluorescence assays (IFAs) and Western blots were performed as described previously (28). For IFAs, we used monoclonal rat anti-HA (1:500 dilution; clone 3F10, Roche) and monoclonal mouse anti-*Tg*P30 (1:1000; clone TP3, Abcam, catalog no. ab8313) as primary antibodies and anti-mouse Alexa Fluor 546 (1:500; Thermo Fisher, catalog no. A-11030), anti-mouse Alexa Fluor 488 (1:500; Thermo Fisher, catalog no. A-11029), and anti-rat Alexa Fluor 488 (1:200; Thermo Fisher, catalog no. A-11006) as secondary antibodies. Microscopy was performed on a DeltaVision Elite system (GE Healthcare) using an inverted IX71 microscope with a ×100 UPlanSApo oil immersion lens (Olympus). Images were taken using a Photometrics CoolSNAP HQ^2 camera and deconvolved and adjusted for contrast and brightness using SoftWoRx Suite 2.0 software. For Western blotting, we used monoclonal rat anti-HA (1:500 dilution; clone 3F10, Roche) and mouse anti-GRA8 (1:10,000 dilution; a kind gift from Gary Ward, University of Vermont

[7] Please note that the JBC is not responsible for the long-term archiving and maintenance of this site or any other third party–hosted site.

(55)) as primary antibodies and horse radish peroxidase–conjugated goat anti-rat (1:5000 dilution; Santa Cruz Biotechnology, catalog no. sc-2006) and goat anti-mouse (1:10,000 dilution; Santa Cruz Biotechnology, catalog no. sc-2005) as secondary antibodies.

Parasite growth, invasion, egress, viability, and virulence assays

Fluorometic *T. gondii* growth assays were performed as described previously (32). The parasites used in the experiments shown in Fig. 2*D* had egressed naturally 2–12 h prior to setting up the assays. Plaque assays were performed as described previously (28), except that 2000 parasites were added per flask. For intracellular growth assays, infected host cells were washed in a high-$[K^+]$ "intracellular" buffer (125 mM KCl, 5 mM NaCl, 25 mM HEPES, 20 mM glucose, and 1 mM $MgCl_2$ (pH 7.4)). Parasites were then mechanically released from host cells by passing infected cells through a 26-gauge needle. Released parasites were filtered through a 3-μm filter and incubated on human foreskin fibroblast–containing coverslips for 1 h. The intracellular buffer was removed by aspiration and replaced with DMEM. Parasites were incubated a further 4 h, during which they were able to invade host cells; then parasites that had failed to invade were removed by washing the host cells three times in DMEM. Infected host cells were cultured for a further 20 h before fixation and counting of the number of parasites in vacuoles. Parasites within at least 100 vacuoles were counted for each condition.

Parasites for invasion assays were prepared as for the intracellular growth assays, except that parasites were incubated in the presence of DMEM for 10 min to allow invasion into host cells. Parasites were fixed in a solution of 3% (v/v) paraformaldehyde and 0.1% (v/v) glutaraldehyde in PBS. Extracellular parasites were labeled with monoclonal mouse anti-*Tg*P30 (1:1000; clone TP3, Abcam, catalog no. ab8313) as a primary antibody and anti-mouse Alexa Fluor 488 (1:500; Thermo Fisher, catalog no. A-11029) as a secondary antibody. At least 100 parasites encompassing 10–15 fields of view were counted for each assay.

Egress assays were performed as described previously (29). Briefly, parasites were allowed to invade host cells for 1 h, and then parasites that had not invaded were removed by washing the host cells three times with DMEM. Parasites were then grown with or without ATc (0.5 μg/ml) for 30 h. The culture medium was removed, infected host cells were washed three times with DMEM, and stimulation medium (DMEM supplemented with 10 mM HEPES and 2 μM A23187 (Sigma-Aldrich)) was added to induce egress. After 3 min, parasites were fixed using 4% (v/v) paraformaldehyde in PBS and stained for IFAs using the primary antibody rabbit anti-GAP45 (1:500 dilution, a kind gift from Con Beckers, University of North Carolina). Co-staining was performed with rat anti-HA to confirm the reduced expression of HA-*Tg*ATP4. Parasitophorous vacuoles were counted using the fluorescence resulting from GAP45 staining. Egress was considered to have occurred from a vacuole when at least one parasite was observed to have escaped.

To measure the viability of extracellular parasites, iHA-*Tg*ATP4 and WT parasites were grown in the absence or presence of ATc for 2 days. Flasks containing infected host cells were washed once in growth medium to remove extracellular parasites, and then parasites were mechanically egressed from host cells by passage through a 26-gauge needle. The released parasites were filtered through a 3-μm filter to remove host cell debris and then incubated for 27 h in growth medium in a humidified 5% CO_2 incubator set to 37 °C. Parasite samples were taken at 0, 4, 9, 20, and 27 h, pelleted by centrifugation at 12,000 × *g* for 1 min, and then resuspended in a solution of 1 μg/ml propidium iodide in PBS supplemented with 10 mM D-glucose. Samples were incubated at room temperature in the dark for 20 min and then analyzed by flow cytometry on an LSR II flow cytometer (BD Biosciences). Viable parasites were gated based on forward scatter, side scatter, and propidium iodide fluorescence and analyzed using FlowJo software.

To measure the effects of the disruption of the *TgATP4* gene on parasite virulence, we infected five 6- to 8-week-old female BALB/c mice with 10^3 WT (RHΔhxprt/Tomato), $atp4^{\Delta 34-1338}$, or $atp4^{\Delta 34-1338}$/cTy1-*Tg*ATP4 parasites. Parasites were intracellular at the time of preparation and were manually egressed by passage through a 26-gauge needle. After centrifugation at 1500 × *g* for 10 min to sediment the parasites, the parasites were resuspended in PBS and injected into mice within 1 h of egress. Mice were monitored daily for symptoms of toxoplasmosis, and those exhibiting terminal symptoms were euthanized.

Fluorometric ion measurements

iHA-*Tg*ATP4 parasites, grown in 175-cm^2 tissue culture flasks for 2 days in the presence of either ATc (0.5 μg/ml) or solvent (0.025% (v/v) ethanol), were harvested by passage of cultures through a 26-gauge needle. The parasites were then passed through a 3-μm filter to remove host cell debris and centrifuged at 1500 × *g* for 10 min. The supernatant medium was removed, and the parasites were resuspended in 1 ml of physiological saline (125 mM NaCl, 5 mM KCl, 25 mM HEPES, 20 mM glucose, and 1 mM $MgCl_2$ (pH 7.10)) and then centrifuged at 12,000 × *g* for 1 min. The supernatant solution was removed, and the parasites were resuspended again in physiological saline to which the appropriate fluorescent dye was added.

$[Na^+]_{cyt}$, pH_{cyt}, and $[Ca^{2+}]_{cyt}$ were measured using the Na^+-sensitive dye SBFI, the pH-sensitive dye BCECF, and the Ca^{2+}-sensitive dye Fura-2, respectively. In all cases, parasites were suspended in physiological saline and loaded using the acetoxymethyl ester forms of the dyes (Molecular Probes) at 37 °C. In the case of SBFI, parasites were loaded with 6 μM SBFI for 30 min in the presence of 0.1% w/v Pluronic F-127. For BCECF, parasites were loaded for 14 min in the absence of Pluronic F-127, and the BCECF concentration was 5 μM. For Fura-2, loading was performed over 30 min using 6 μM Fura-2 and 0.04% (w/v) Pluronic F-127. The parasites were washed twice after dye loading to remove extracellular dye.

In all cases, fluorescence measurements were performed at 37 °C on 5–10 × 10^7 parasites using a PerkinElmer LS 50B fluorescence spectrometer with a dual excitation Fast Filter accessory. Measurements were taken every 0.6 s, and a 6-s roll-

ing average was applied to the data shown in Figs. 5, 6, *B* and *C*, and 7*A*. In Figs. 5, 6, *B* and *C*, and 7*A*, the parasites were suspended in physiological saline for the fluorescence measurements. In Fig. 7*B*, parasites were suspended in a solution that was identical to physiological saline except that it contained 1 mM EGTA (Ca^{2+}-free saline solution) or in Ca^{2+}-free saline solution to which had been added sufficient $CaCl_2$ to achieve a final free [Ca^{2+}] of 1,100 or 1,000 μM (Ca-EGTA Calculator v1.3).

For $[Na^+]_{cyt}$ and $[Ca^{2+}]_{cyt}$ experiments, the dye-loaded cells were excited at 340 nm and 380 nm, with fluorescence measured at 515 nm. For pH_{cyt} experiments, the excitation wavelengths were 440 nm and 495 nm, and the emission wavelength was 520 nm. $[Ca^{2+}]_{cyt}$ measurements were calibrated *in situ* (56) using a K_d of 120 nM for the Fura-2/Ca^{2+} complex. pH_{cyt} measurements were calibrated as described previously (3). Cell number limitations prevented full calibration of Na^+ measurements; however, the fluorescence ratios corresponding to 130 mM Na^+ and 20 mM Na^+ were determined, essentially as described previously (57, 58), by suspending parasites in calibration salines containing either 130 mM or 20 mM Na^+ and adding the ionophores gramicidin, nigericin, and monensin (each at 4 μM). Segments of the calibration traces are shown before the time courses presented in Figs. 5*A* and 6*B*.

HPLC measurements

An HPLC-based method described previously (11) for analysis of intracellular Na^+ and K^+ content in *Plasmodium* parasites was adapted here for use with *T. gondii*. Parasites were harvested by passage of cultures through a 26-gauge needle. The parasites were then passed through a 3-μm filter to remove host cell debris and centrifuged at 1500 × *g* for 10 min. The supernatant medium was removed, and the parasites were washed and resuspended in a saline solution and then incubated with cipargamin or DMSO (the conditions tested are detailed in the legend for Fig. S5). The parasites were then sedimented by centrifugation and washed three times (12,000 × *g*, 1 min) in ice-cold wash buffer (150 mM magnesium acetate (pH 7.1)). The parasites were then resuspended in 100 μl of lysis buffer (40%/60% (v/v) 20 mM ammonium acetate (pH 5)/acetonitrile) and centrifuged (16,000 × *g*, 5 min) to remove insoluble matter. The supernatant solution was transferred into a vial for HPLC analysis, which was performed as described previously (11).

Statistics

Data were tested for statistical significance using *t* tests (two-tailed, unpaired) or one-way ANOVA, as stated in the relevant sections. For the fluorescence-based assays of parasite growth (for which data are shown in Fig. 2*D*), one-way ANOVA was performed on the prenormalized data (fluorescence intensity units, after subtraction of the background), and "experiment" was used as a "blocking factor" to prevent any differences in fluorescence intensity between different experiments from eroding the precision of the test. *Post hoc* comparisons were then performed using the least significant difference test. For one-way ANOVAs performed without blocking, a *post hoc* Tukey test was used.

Author contributions—A. M. L., A. S. M. D., K. K., and G. G. v. D. conceptualization; A. M. L., A. S. M. D., K. O. B., D. L., E. R., J. M. M., H. M. M., M. W., F. R., C. J. T., and G. G. v. D. formal analysis; A. M. L., C. J. T., K. K., and G. G. v. D. supervision; A. M. L., C. J. T., K. K., and G. G. v. D. funding acquisition; A. M. L., A. S. M. D., K. O. B., D. L., E. R., J. M. M., H. M. M., M. W., F. R., and G. G. v. D. investigation; A. M. L., K. K., and G. G. v. D. writing-original draft; A. M. L., K. K., and G. G. v. D. project administration; A. S. M. D., K. O. B., D. L., E. R., J. M. M., H. M. M., M. W., F. R., and C. J. T. writing-review and editing.

Acknowledgments—We thank Akhil Vaidya and the Medicines for Malaria Venture for the provision of PA21A050 and cipargamin, respectively.

References

1. Blaustein, M. P., Kao, J. P., and Matteson, D. R. (2004) *Cellular Physiology*, pp. 37–52 Elsevier, Philadelphia, PA
2. Casey, J. R., Grinstein, S., and Orlowski, J. (2010) Sensors and regulators of intracellular pH. *Nat. Rev. Mol. Cell Biol.* **11,** 50–61 CrossRef Medline
3. Saliba, K. J., and Kirk, K. (1999) pH regulation in the intracellular malaria parasite, *Plasmodium falciparum*: H^+ extrusion via a V-type H^+-ATPase. *J. Biol. Chem.* **274,** 33213–33219 CrossRef Medline
4. Spillman, N. J., Allen, R. J., and Kirk, K. (2008) Acid extrusion from the intraerythrocytic malaria parasite is not via a Na^+/H^+ exchanger. *Mol. Biochem. Parasitol.* **162,** 96–99 CrossRef Medline
5. Allen, R. J., and Kirk, K. (2004) The membrane potential of the intraerythrocytic malaria parasite *Plasmodium falciparum*. *J. Biol. Chem.* **279,** 11264–11272 CrossRef Medline
6. Moreno, S. N., Zhong, L., Lu, H. G., Souza, W. D., and Benchimol, M. (1998) Vacuolar-type H^+-ATPase regulates cytoplasmic pH in *Toxoplasma gondii* tachyzoites. *Biochem. J.* **330,** 853–860 CrossRef Medline
7. Rottmann, M., McNamara, C., Yeung, B. K., Lee, M. C., Zou, B., Russell, B., Seitz, P., Plouffe, D. M., Dharia, N. V., Tan, J., Cohen, S. B., Spencer, K. R., González-Páez, G. E., Lakshminarayana, S. B., Goh A., *et al.* (2010) Spiroindolones, a potent compound class for the treatment of malaria. *Science* **329,** 1175–1180 CrossRef Medline
8. Krishna, S., Woodrow, C., Webb, R., Penny, J., Takeyasu, K., Kimura, M., and East, J. M. (2001) Expression and functional characterization of a *Plasmodium falciparum* Ca^{2+}-ATPase (PfATP4) belonging to a subclass unique to apicomplexan organisms. *J. Biol. Chem.* **276,** 10782–10787 CrossRef Medline
9. Dennis, A. S. M., Lehane, A. M., Ridgway, M. C., Holleran, J. P., and Kirk, K. (2018) Cell swelling induced by the antimalarial KAE609 (cipargamin) and other PfATP4-associated antimalarials. *Antimicrob. Agents Chemother.* **62,** e00087-18 Medline
10. Spillman, N. J., Allen, R. J., McNamara, C. W., Yeung, B. K., Winzeler, E. A., Diagana, T. T., and Kirk, K. (2013) Na^+ regulation in the malaria parasite *Plasmodium falciparum* involves the cation ATPase PfATP4 and is a target of the spiroindolone antimalarials. *Cell Host Microbe* **13,** 227–237 CrossRef Medline
11. Winterberg, M., and Kirk, K. (2016) A high-sensitivity HPLC assay for measuring intracellular Na^+ and K^+ and its application to *Plasmodium falciparum* infected erythrocytes. *Sci. Rep.* **6,** 29241 CrossRef Medline
12. Flannery, E. L., McNamara, C. W., Kim, S. W., Kato, T. S., Li, F., Teng, C. H., Gagaring, K., Manary, M. J., Barboa, R., Meister, S., Kuhen, K., Vinetz, J. M., Chatterjee, A. K., and Winzeler, E. A. (2015) Mutations in the P-type cation-transporter ATPase 4, PfATP4, mediate resistance to both aminopyrazole and spiroindolone antimalarials. *ACS Chem. Biol.* **10,** 413–420 CrossRef Medline
13. Jiménez-Díaz, M. B., Ebert, D., Salinas, Y., Pradhan, A., Lehane, A. M., Myrand-Lapierre, M. E., O'Loughlin, K. G., Shackleford, D. M., Justino de Almeida, M., Carrillo, A. K., Clark, J. A., Dennis, A. S., Diep, J., Deng, X., Duffy S., *et al.* (2014) (+)-SJ733, a clinical candidate for malaria that acts

through ATP4 to induce rapid host-mediated clearance of *Plasmodium*. *Proc. Natl. Acad. Sci. U.S.A.* **111,** E5455–E5462 CrossRef Medline
14. Lehane, A. M., Ridgway, M. C., Baker, E., and Kirk, K. (2014) Diverse chemotypes disrupt ion homeostasis in the malaria parasite. *Mol. Microbiol.* **94,** 327–339 CrossRef Medline
15. Vaidya, A. B., Morrisey, J. M., Zhang, Z., Das, S., Daly, T. M., Otto, T. D., Spillman, N. J., Wyvratt, M., Siegl, P., Marfurt, J., Wirjanata, G., Sebayang, B. F., Price, R. N., Chatterjee, A., Nagle A., *et al.* (2014) Pyrazoleamide compounds are potent antimalarials that target Na^+ homeostasis in intraerythrocytic *Plasmodium falciparum*. *Nat. Commun.* **5,** 5521 CrossRef Medline
16. Dennis, A. S. M., Rosling, J. E. O., Lehane, A. M., and Kirk, K. (2018) Diverse antimalarials from whole-cell phenotypic screens disrupt malaria parasite ion and volume homeostasis. *Sci. Rep.* **8,** 8795 CrossRef Medline
17. Rosling, J. E. O., Ridgway, M. C., Summers, R. L., Kirk, K., and Lehane, A. M. (2018) Biochemical characterization and chemical inhibition of PfATP4-associated Na^+-ATPase activity in *Plasmodium falciparum* membranes. *J. Biol. Chem.* **293,** 13327–13337 CrossRef Medline
18. Hewitt, S. N., Dranow, D. M., Horst, B. G., Abendroth, J. A., Forte, B., Hallyburton, I., Jansen, C., Baragaña, B., Choi, R., Rivas, K. L., Hulverson, M. A., Dumais, M., Edwards, T. E., Lorimer, D. D., Fairlamb, A. H., *et al.* (2017) Biochemical and structural characterization of selective allosteric inhibitors of the *Plasmodium falciparum* drug target, prolyl-tRNA-synthetase. *ACS Infect. Dis.* **3,** 34–44 CrossRef Medline
19. Spillman, N. J., Allen, R. J., and Kirk, K. (2013) Na^+ extrusion imposes an acid load on the intraerythrocytic malaria parasite. *Mol. Biochem. Parasitol.* **189,** 1–4 CrossRef Medline
20. Das, S., Bhatanagar, S., Morrisey, J. M., Daly, T. M., Burns, J. M., Jr, Coppens, I., and Vaidya, A. B. (2016) Na^+ influx induced by new antimalarials causes rapid alterations in the cholesterol content and morphology of *Plasmodium falciparum*. *PLoS Pathog.* **12,** e1005647 CrossRef Medline
21. Arrizabalaga, G., Ruiz, F., Moreno, S., and Boothroyd, J. C. (2004) Ionophore-resistant mutant of *Toxoplasma gondii* reveals involvement of a sodium/hydrogen exchanger in calcium regulation. *J. Cell Biol.* **165,** 653–662 CrossRef Medline
22. Francia, M. E., Wicher, S., Pace, D. A., Sullivan, J., Moreno, S. N., and Arrizabalaga, G. (2011) A *Toxoplasma gondii* protein with homology to intracellular type Na^+/H^+ exchangers is important for osmoregulation and invasion. *Exp. Cell Res.* **317,** 1382–1396 CrossRef Medline
23. Zhou, Y., Fomovska, A., Muench, S., Lai, B. S., Mui, E., and McLeod, R. (2014) Spiroindolone that inhibits PfATPase4 is a potent, cidal inhibitor of *Toxoplasma gondii* tachyzoites *in vitro* and *in vivo*. *Antimicrob. Agents Chemother.* **58,** 1789–1792 CrossRef Medline
24. Axelsen, K. B., and Palmgren, M. G. (1998) Evolution of substrate specificities in the P-type ATPase superfamily. *J. Mol. Evol.* **46,** 84–101 CrossRef Medline
25. Cavalier-Smith, T., and Chao, E. E. (2004) Protalveolate phylogeny and systematics and the origins of Sporozoa and dinoflagellates (phylum Myzozoa nom. nov.). *Eur. J. Protistol.* **40,** 185–212 CrossRef
26. Moore, R. B., Oborník, M., Janouskovec, J., Chrudimský, T., Vancová, M., Green, D. H., Wright, S. W., Davies, N. W., Bolch, C. J., Heimann, K., Slapeta, J., Hoegh-Guldberg, O., Logsdon, J. M., and Carter, D. A. (2008) A photosynthetic alveolate closely related to apicomplexan parasites. *Nature* **451,** 959–963 CrossRef Medline
27. Sibley, L. D., Krahenbuhl, J. L., Adams, G. M., and Weidner, E. (1986) *Toxoplasma* modifies macrophage phagosomes by secretion of a vesicular network rich in surface proteins. *J. Cell Biol.* **103,** 867–874 CrossRef Medline
28. van Dooren, G. G., Tomova, C., Agrawal, S., Humbel, B. M., and Striepen, B. (2008) *Toxoplasma gondii* Tic20 is essential for apicoplast protein import. *Proc. Natl. Acad. Sci. U.S.A.* **105,** 13574–13579 CrossRef Medline
29. McCoy, J. M., Whitehead, L., van Dooren, G. G., and Tonkin, C. J. (2012) *Tg*CDPK3 regulates calcium-dependent egress of *Toxoplasma gondii* from host cells. *PLoS Pathog.* **8,** e1003066 CrossRef Medline
30. Joyce, B. R., Queener, S. F., Wek, R. C., and Sullivan, W. J., Jr. (2010) Phosphorylation of eukaryotic initiation factor-2α promotes the extracellular survival of obligate intracellular parasite *Toxoplasma gondii*. *Proc. Natl. Acad. Sci. U.S.A.* **107,** 17200–17205 CrossRef Medline
31. Borel, E., Mayençon, M., Kaiser, K., Picot, S., and Peyron, F. (1998) Fluorogenic detection of viable *Toxoplasma gondii*. *Parasite* **5,** 371–373 CrossRef Medline
32. Rajendran, E., Hapuarachchi, S. V., Miller, C. M., Fairweather, S. J., Cai, Y., Smith, N. C., Cockburn, I. A., Bröer, S., Kirk, K., and van Dooren, G. G. (2017) Cationic amino acid transporters play key roles in the survival and transmission of apicomplexan parasites. *Nat. Commun.* **8,** 14455 CrossRef Medline
33. Dyer, M., Jackson, M., McWhinney, C., Zhao, G., and Mikkelsen, R. (1996) Analysis of a cation-transporting ATPase of *Plasmodium falciparum*. *Mol. Biochem. Parasitol.* **78,** 1–12 CrossRef Medline
34. Trottein, F., Thompson, J., and Cowman, A. F. (1995) Cloning of a new cation ATPase from *Plasmodium falciparum*: conservation of critical amino acids involved in calcium binding in mammalian organellar Ca^{2+}-ATPases. *Gene* **158,** 133–137 CrossRef Medline
35. Rodríguez-Navarro, A., and Benito, B. (2010) Sodium or potassium efflux ATPase a fungal, bryophyte, and protozoal ATPase. *Biochim. Biophys. Acta* **1798,** 1841–1853 CrossRef Medline
36. Miranda, K., Pace, D. A., Cintron, R., Rodrigues, J. C. F., Fang, J., Smith, A., Rohloff, P., Coelho, E., de Haas, F., de Souza, W., Coppens, I., Sibley, L. D., and Moreno, S. N. (2010) Characterization of a novel organelle in *Toxoplasma gondii* with similar composition and function to the plant vacuole. *Mol. Microbiol.* **76,** 1358–1375 CrossRef Medline
37. Goldgof, G. M., Durrant, J. D., Ottilie, S., Vigil, E., Allen, K. E., Gunawan, F., Kostylev, M., Henderson, K. A., Yang, J., Schenken, J., LaMonte, G. M., Manary, M. J., Murao, A., Nachon, M., Stanhope, R., *et al.* (2016) Comparative chemical genomics reveal that the spiroindolone antimalarial KAE609 (cipargamin) is a P-type ATPase inhibitor. *Sci. Rep.* **6,** 27806 CrossRef Medline
38. Van Voorhis, W. C., Adams, J. H., Adelfio, R., Ahyong, V., Akabas, M. H., Alano, P., Alday, A., Alemán Resto, Y., Alsibaee, A., Alzualde, A., Andrews, K. T., Avery, S. V., Avery, V. M., Ayong, L., Baker, M., *et al.* (2016) Open source drug discovery with the Malaria Box compound collection for neglected diseases and beyond. *PLoS Pathog.* **12,** e1005763 CrossRef Medline
39. Kirk, K. (2015) Ion regulation in the malaria parasite. *Annu. Rev. Microbiol.* **69,** 341–359 CrossRef Medline
40. Lee, P., Ye, Z., Van Dyke, K., and Kirk, R. G. (1988) X-ray-microanalysis of *Plasmodium falciparum* and infected red blood cells: effects of qinghaosu and chloroquine on potassium, sodium, and phosphorus composition. *Am. J. Trop. Med. Hyg.* **39,** 157–165 CrossRef Medline
41. Mauritz, J. M., Seear, R., Esposito, A., Kaminski, C. F., Skepper, J. N., Warley, A., Lew, V. L., and Tiffert, T. (2011) X-ray microanalysis investigation of the changes in Na, K, and hemoglobin concentration in *Plasmodium falciparum*-infected red blood cells. *Biophys. J.* **100,** 1438–1445 CrossRef Medline
42. Staines, H. M., Ellory, J. C., and Kirk, K. (2001) Perturbation of the pump-leak balance for Na^+ and K^+ in malaria-infected erythrocytes. *Am. J. Physiol. Cell Phys.* **280,** C1576–C1587 CrossRef Medline
43. Sidik, S. M., Huet, D., Ganesan, S. M., Huynh, M. H., Wang, T., Nasamu, A. S., Thiru, P., Saeij, J. P. J., Carruthers, V. B., Niles, J. C., and Lourido, S. (2016) A genome-wide CRISPR screen in *Toxoplasma* identifies essential apicomplexan genes. *Cell* **166,** 1423–1435.e12 CrossRef Medline
44. van Dooren, G. G., and Striepen, B. (2013) The algal past and parasite present of the apicoplast. *Annu. Rev. Microbiol.* **67,** 271–289 CrossRef Medline
45. Barnes, H. (1954) Some tables for the ionic composition of sea water. *J. Exp. Biol.* **31,** 582–588
46. Thompson, J. D., Gibson, T. J., Plewniak, F., Jeanmougin, F., and Higgins, D. G. (1997) The CLUSTAL_X windows interface: flexible strategies for multiple sequence alignment aided by quality analysis tools. *Nucleic Acids Res.* **25,** 4876–4882 CrossRef Medline
47. Shoguchi, E., Shinzato, C., Kawashima, T., Gyoja, F., Mungpakdee, S., Koyanagi, R., Takeuchi, T., Hisata, K., Tanaka, M., Fujiwara, M., Hamada, M., Seidi, A., Fujie, M., Usami, T., Goto, H., *et al.* (2013) Draft assembly of the *Symbiodinium minutum* nuclear genome reveals dinoflagellate gene structure. *Curr. Biol.* **23,** 1399–1408 CrossRef Medline

48. Gornik, S. G., Febrimarsa Cassin, A. M., MacRae, J. I., Ramaprasad, A., Rchiad, Z., McConville, M. J., Bacic, A., McFadden, G. I., Pain, A., and Waller, R. F. (2015) Endosymbiosis undone by stepwise elimination of the plastid in a parasitic dinoflagellate. *Proc. Natl. Acad. Sci. U.S.A.* **112,** 5767–5772 CrossRef Medline
49. Foth, B. J. (2007) Phylogenetic analysis to uncover organellar origins of nuclear-encoded genes. *Methods Mol. Biol.* **390,** 467–488 CrossRef Medline
50. Sheiner, L., Demerly, J. L., Poulsen, N., Beatty, W. L., Lucas, O., Behnke, M. S., White, M. W., and Striepen, B. (2011) A systematic screen to discover and analyze apicoplast proteins identifies a conserved and essential protein import factor. *PLoS Pathog.* **7,** e1002392 CrossRef Medline
51. Striepen, B., and Soldati, D. (2007) In *Toxoplasma gondii: The Model Apicomplexan: Perspectives and Methods* (Weiss, L. D., and Kim, K., eds) pp. 391–415, Elsevier, London
52. Katris, N. J., van Dooren, G. G., McMillan, P. J., Hanssen, E., Tilley, L., and Waller, R. F. (2014) The apical complex provides a regulated gateway for secretion of invasion factors in *Toxoplasma*. *PLoS Pathog.* **10,** e1004074 CrossRef Medline
53. van Dooren, G. G., Yeoh, L. M., Striepen, B., and McFadden, G. I. (2016) The import of proteins into the mitochondrion of *Toxoplasma gondii*. *J. Biol. Chem.* **291,** 19335–19350 CrossRef Medline
54. Shen, B., Brown, K. M., Lee, T. D., and Sibley, L. D. (2014) Efficient gene disruption in diverse strains of *Toxoplasma gondii* using CRISPR/CAS9. *MBio* **5,** e01114-14 Medline
55. Carey, K. L., Donahue, C. G., and Ward, G. E. (2000) Identification and molecular characterization of GRA8, a novel, proline-rich, dense granule protein of *Toxoplasma gondii*. *Mol. Biochem. Parasitol.* **105,** 25–37 CrossRef Medline
56. Grynkiewicz, G., Poenie, M., and Tsien, R. Y. (1985) A new generation of Ca^{2+} indicators with greatly improved fluorescence properties. *J. Biol. Chem.* **260,** 3440–3450 Medline
57. Diarra, A., Sheldon, C., and Church, J. (2001) *In situ* calibration and $[H^+]$ sensitivity of the fluorescent Na^+ indicator SBFI. *Am. J. Physiol. Cell Physiol.* **280,** C1623–1633 CrossRef Medline
58. Harootunian, A. T., Kao, J. P., Eckert, B. K., and Tsien, R. Y. (1989) Fluorescence ratio imaging of cytosolic free Na^+ in individual fibroblasts and lymphocytes. *J. Biol. Chem.* **264,** 19458–19467 Medline
59. Alleva, L. M., and Kirk, K. (2001) Calcium regulation in the intraerythrocytic malaria parasite *Plasmodium falciparum*. *Mol. Biochem. Parasitol.* **117,** 121–128 CrossRef Medline

Characterization of the ATP4 ion pump in *Toxoplasma gondii*

Adele M. Lehane, Adelaide S. M. Dennis, Katherine O. Bray, Dongdi Li, Esther Rajendran, James M. McCoy, Hillary M. McArthur, Markus Winterberg, Farid Rahimi, Christopher J. Tonkin, Kiaran Kirk and Giel G. van Dooren

J. Biol. Chem. 2019, 294:5720-5734.
doi: 10.1074/jbc.RA118.006706 originally published online February 5, 2019
